数理解析研究所講究録 1210 巻 2001 年 68-77

Modeling of Grain Structure Evolution

R.Kobayashi
Research Institute for Electronic Science, Hokkaido University
北海道大学電子科学研究所　小林 亮

Abstract

Two dimensional frame-inveriant phase field model of grain boundaries is developed. The essential feture of the models is that it can simulate grain boundary motion and grain rotation simultaneously. Also it is conbined with the solidification model to construct models which describes the whole process - solidification from nuclei, impingement of crystals, formation of grain boundary and the following grain structure evolution.

1 Introduction

The study of grain boundary formation and the following evolution process is quite important in materials science. All the polycrystalline materials have grain boundaries, and the behavior of these interfaces can have an enormous influence on the properties of the materials. Thus, over the years, a great deal of intellectual effort has been applied to deriving models of the formation of grain boundaries and their subsequent evolution.

Previously we presented a phase field model and simulations of the simultaneous processes of solidification and impingement of arbitrarily oriented crystals, yielding an incipient two dimensional grain structure [1]. A model which attempted to address the subsequent coarsening of impinged grains was presented in [2]. In other attempts to model this phenomenon a finite number of crystalline orientations are allowed with respect to the fixed coordinate reference frame. Morin et al.[3], and Lusk [4] constructed a free energy density having N minima by introducing a rotational (orientation) variable in the homogeneous free energy. Chen and Yang[5] and

Steinbach et al.[6] assigned N order parameters to the N allowed orientations. In these approaches, the free energy density depends on the orientation of the crystal measured in the fixed frame—a property which is not physical.

Recently we presented a new phase field model of grain structure evolution [8]. The essential feature of our new model are that (1) the homogeneous part of the free energy density is reference frame-invariant; (2) the spatial extent of regions where the crystallographic orientational order changes (i.e., a grain boundary) is finite, stable in time, and determined by model parameters; (3) grain boundaries evolve by both boundary motion and reduction of misorientation energy (rotation).

In addition, we will demonstrate an extended model which can describe the solidification, formation of grain boundary and the following evolution of grain structure.

2 Isotropic η-θ Model

2.1 Modeling

Let us consider the situation that the whole region is already solidified and filled with a number of grains. The model parameters, η, and θ, represent: a coarse-grained measure of the degree of crystalline order, and the crystalline orientation, respectively. For precise interpretations of η and θ, consider a fixed subregion of solid material. At the atomic scale, a discrete variable θ_i, representing the orientation of an atomic bond (lattice vector) with respect to some fixed laboratory frame, is proposed. For a subregion that defines a coarse-graining scale, we define η and θ such that

$$(\eta\cos\theta, \eta\sin\theta) = \frac{1}{N}\sum_{i=1}^{N}(\cos\theta_i, \sin\theta_i), \tag{2.1}$$

where N is the number of bonds in the subregion. The variable η is an order parameter for the degree of crystalline orientational order, where $\eta = 1$ signifies a completely oriented state and $\eta = 0$ a state where no meaningful value of orientation exists in the subregion, and $0 \leq \eta \leq 1$ always holds. The variable θ is an indicator of the mean orientation of the crystalline subregion. Note, that when symmetrically

equivalent crystalline directions exist, θ may not be uniquely defined. However, the point group symmetry operations can be used to map each of the θ_i into a sub-domain of $(0, 2\pi)$ where they are unique.

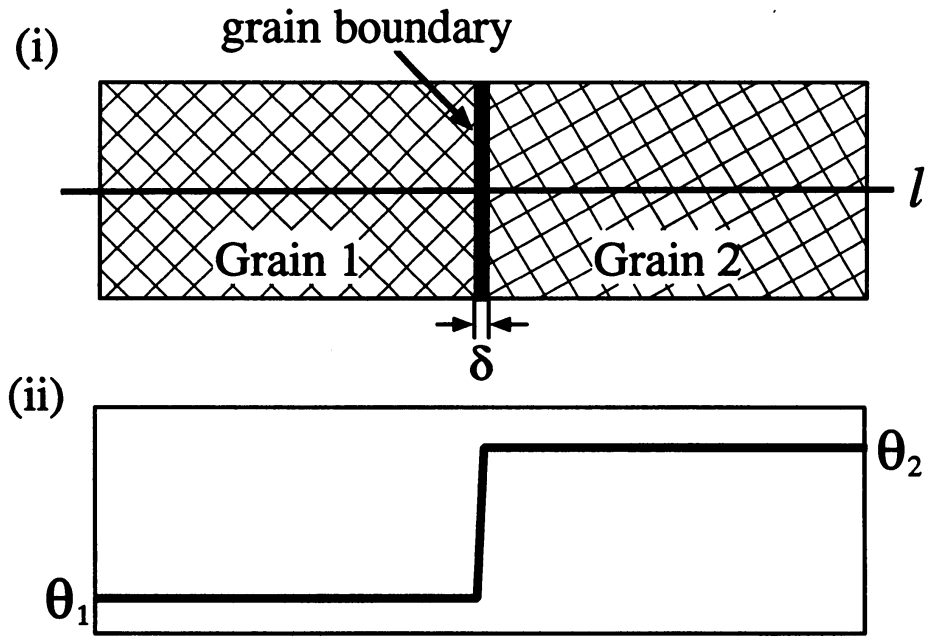

Figure 2.1: (i) Schematic drawing of bicrystal. (ii) Graph of angle variable θ measured along the line l.

Consider a bicrystal with a single grain boundary as indicated in Fig.2.1(a), and fix the crystallographic orientation at each end to be θ_1 and θ_2 respectively. Dirichlet conditions are imposed for the purpose of understanding grain boundary energy and structure (i.e., $\theta(x)$ and $\eta(x)$) in a finite domain $0 \leq x \leq L$. Empirical observations indicate that the spatial variation of orientation is such that orientation is uniform over most of the length L (L is assumed to be large enough so that (2.1) applies) and there is transition area where the change in crystallographic orientation is localized to a region $\delta \ll L$ as in Fig.2.1, where δ is the grain boundary width.

In the usual phase field model, or more generally bistable reaction diffusion systems, this kind of front structure is attained by the balance between the dynamical term and the diffusion term, and the values in the bulk are kept constant by the

fact that the values there are stable fixed points of the dynamical term (in this case θ_1 and θ_2). However, by the requirement of rotational invariance, no such special angles should exist and therefore cannot appear in the homogeneous part of the free energy density. Therefore the typical front structure which arises in a bistable reaction diffusion system cannot be used to describe the angle transition across the a grain boundary.

A physical free energy density must result in a localized profile as in Fig.2.1(b), but cannot contain any orientation angles which depend on a particular reference frame. A free energy density that is invariant under rotations of the reference frame can be constructed as follows:

$$E = \frac{1}{\epsilon}\int_\Omega \left[\frac{\nu^2}{2}|\nabla\eta|^2 + f(\eta) + sg(\eta)|\nabla\theta| + \frac{\epsilon^2}{2}h(\eta)|\nabla\theta|^2\right] dA \tag{2.2}$$

with positive parameters ν, s and ϵ. The prefacter $\frac{1}{\epsilon}$ is introduced in order to guarantee that the total enrgy tends to a non-zero constant in the singular limit $\epsilon \to 0$. Simple choices for $f(\eta)$, $g(\eta)$ and $h(\eta)$ are

$$f(\eta) = \frac{1}{2}(1-\eta)^2 \quad \text{and} \quad g(\eta) = h(\eta) = \eta^2. \tag{2.3}$$

The form of $f(\eta)$ is quite reasonable since we assume that only crystalline phase is stable. Without loss of generality, $f(1) = 0$ can be assumed.

Consider η and θ as a polar coordinate system on the unit disk $D = \{\eta \leq 1\}$ as (2.1) suggests, and introduce L^2-norm to the functional space [9]. The equations of motion are

$$\tau_\eta \eta_t = \nu^2\nabla^2\eta - f'(\eta) - sg'(\eta)|\nabla\theta| - \frac{\epsilon^2}{2}h'(\eta)|\nabla\theta|^2, \tag{2.4}$$

$$\tau_\theta \eta^2 \theta_t = \nabla\cdot\left[sg(\eta)\frac{\nabla\theta}{|\nabla\theta|} + \epsilon^2 h(\eta)\nabla\theta\right]. \tag{2.5}$$

where τ_η and τ_θ are inverse mobilities. The form of (2.5) requires careful consideration because it contains a singular diffusivity where $\nabla\theta = 0$. However, this singularity can be treated rigorously and controlled, as shown in [10], [11] and [12].

2.2 1 Dimensional Solutions

Fig.2.2 shows a typical stationary solution corresponding to the situation indicated in Fig.2.1. The flat profile of η in the grain region is due to the fact that $f(\eta)$ has a local minimum at $\eta = 1$, while the graph is pulled down by the 3rd and the 4th term of the right-hand side of (2.4) in the grain boundary region. On the other hand, the flat profile of θ in the grain region is kept by the other mechanism than the one of η. It is the effect of singular diffusivity which is caused by the 1st term of the right-hand side of (2.5).

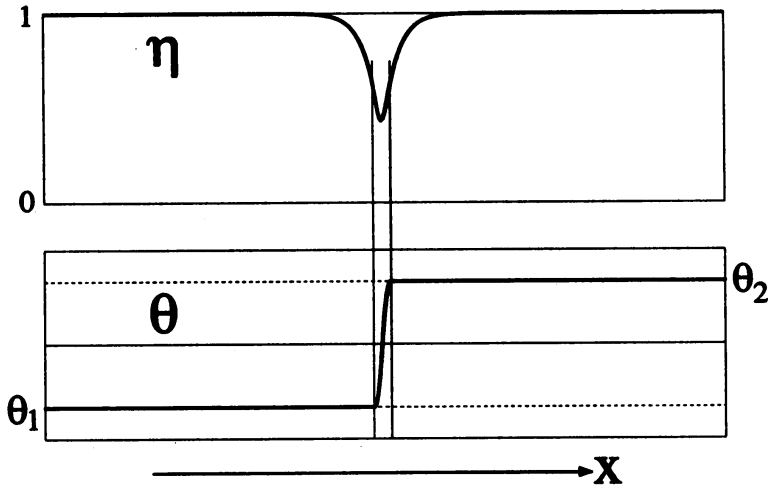

Figure 2.2: 1 dimensional stationary solution with one grain boundary obtained by numerical simulation

The 1st order term of $|\nabla\theta|$ in the energy functional (2.2) strongly penelize the small values of $\nabla\theta$, and prefer to change values in the vicinity of the global minimum of $g(\eta)$. The 2nd order term of $|\nabla\theta|$ permits the small values of $|\nabla\theta|$, while it strongly punish the large values of $|\nabla\theta|$. By the balance of the 1st and 2nd order term, the profile of θ is kept as shown in Fig.2.2.

Quite recently, Lobkovsky and Warren [16] derived the singular limit of our model by setting $\nu = \epsilon\tilde{\nu}$, $s = \epsilon\tilde{s}$, $\tau_\eta = \epsilon^2\tilde{\tau}_\eta$ and $\tau_\theta = \epsilon^2\tilde{\tau}_\theta P(\eta, \epsilon|\nabla\theta|)$. Using the formal expansion they obtain the informations of the stationary solution with one grain

boundary. Fig.2.3 demonstarates the comparison of their theory (solid curves) and the simulated results (square markers), which gives remarkable coincidence between them. They also proved that the grain boundary motion is a motion by mean curvature in the singular limit, which was predicted by numerical simulations in [8]

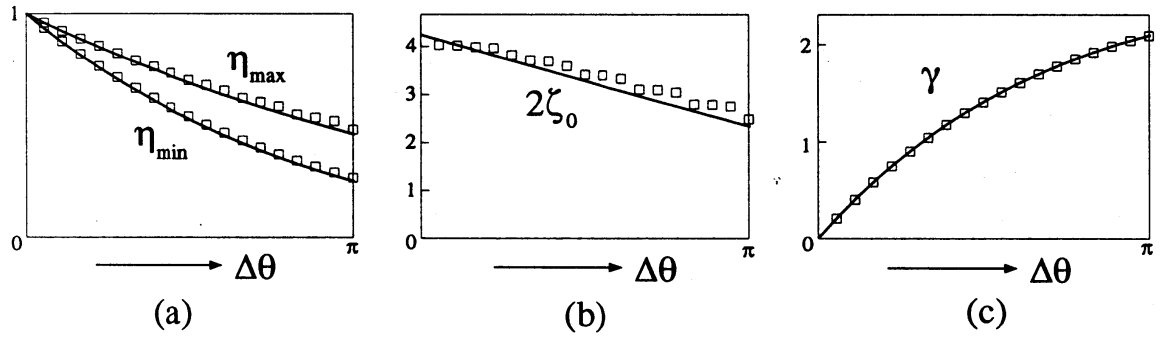

Figure 2.3: All these panels shows the graphs indicating $\Delta\theta$ vs some quantity. The functions $f(\eta) = (1-\eta)^2/2$ and $g(\eta) = h(\eta) = \eta^2$ were used in this culculation. (a) $\eta_{\min}$ is a minimum value of η and $\eta_{\max}$ is a value of η at the connection point between the inner and the outer solution. (b) $2\zeta_0$ is a scaled thickness (scaled by ϵ) of the transition layer of θ. (c) γ is a grain boundary energy given by the limit of (2.2).

2.3 2 Dimensional Simulations

In this subsection we present a two dimensional simulations using the equation system (2.4) and (2.5). In order to control the ratio between the rates of grain boundary motion and grain rotation, we set the time constant τ_θ as $\tau_\theta = \epsilon^2\tilde{\tau}_\theta P(\epsilon|\nabla\theta|)$. Although the form of P in the previous statement with respect to the singular limit was $P(\eta, \epsilon|\nabla\theta|)$, we adopt the simpler form $P(\epsilon|\nabla\theta|)$ as follows;

$$P(\epsilon|\nabla\theta|) = (1-\mu) + \frac{\alpha}{\epsilon}\mu \quad \text{where} \quad \mu = e^{-\beta\epsilon|\nabla\theta|}.$$

Actually μ is an indicator of the grain boundary ($\mu = 0$ implies the grain boundary and $\mu = 1$ does the grain). Therefore $P = 1$ in the grain boundary and $P = \frac{\alpha}{\epsilon}$ in the grain. Grain coarsening is observed throughout the process and, at the same time, some grain boundary disappear by the rotation of grains (not by the motion of grain boundary itself) as shown in Fig. 2.4.

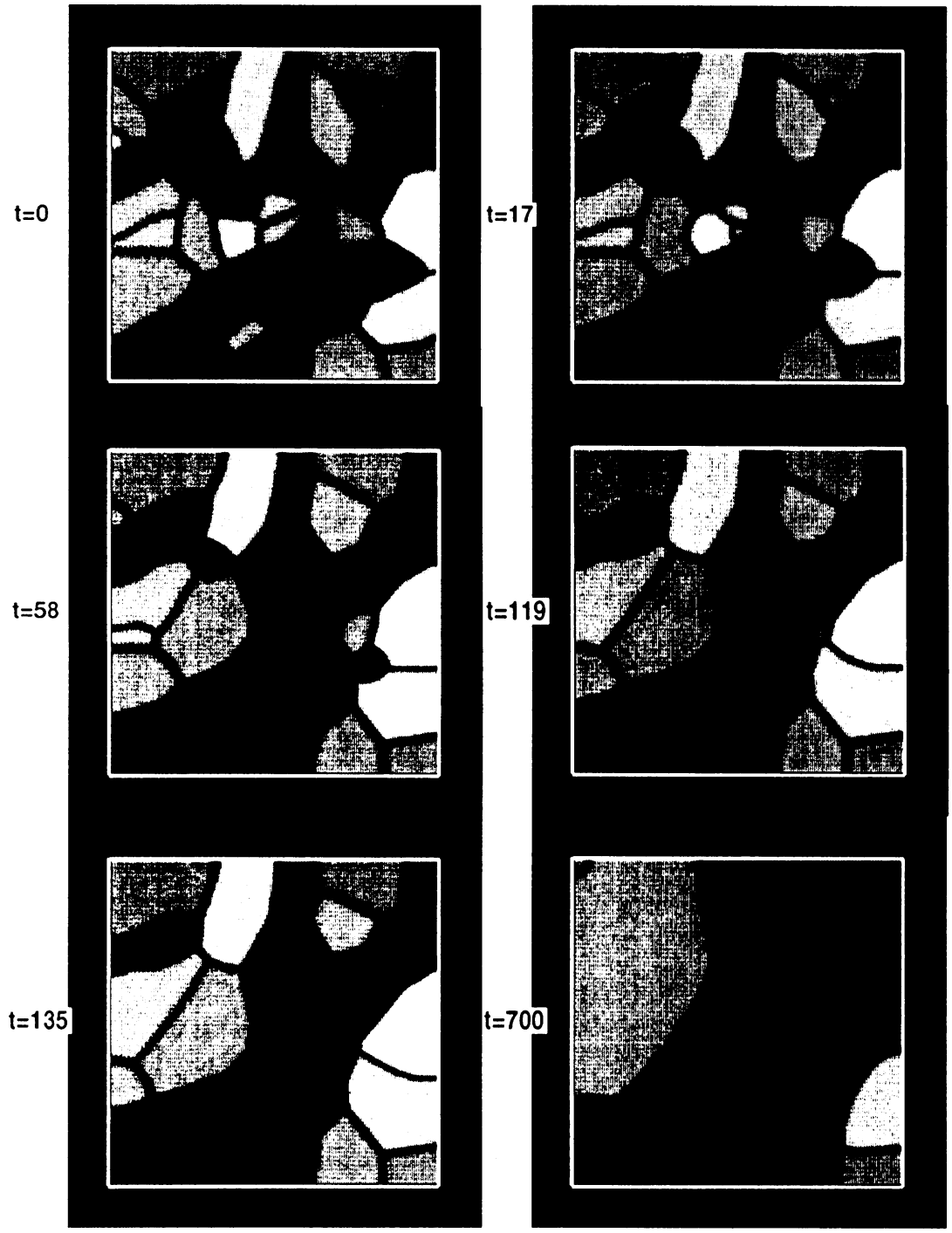

Figure 2.4: Two dimensional simulation of grain coarsening process using functional forms $f(\eta) = (1-\eta)^2/2$, $g(\eta) = \eta^2$ and $h(\eta) = 1$. Neumann boundary conditions are imposed on η and θ.

3 Isotropic ϕ-η-θ Model

3.1 Modeling

In this section we introduce an isotropic model which includes the solidity field ϕ, the orientation ordering field η and the orientation field θ. First, we consider the following energy form as a functional of ϕ, η and θ;

$$E = \int_\Omega \left[\frac{\delta^2}{2}|\nabla\phi|^2 + f(\phi,\eta) + \frac{\nu^2}{2}|\nabla\eta|^2 + s\eta^2|\nabla\theta| + \frac{\epsilon^2}{2}\phi^2|\nabla\theta|^2 \right] dA \tag{3.6}$$

where

$$f(\phi,\eta) = \kappa \int_0^\phi \tilde{\phi}(\tilde{\phi}-1)(\tilde{\phi}-1/2+m)d\tilde{\phi} + \frac{1}{2}(\phi-\eta)^2. \tag{3.7}$$

This potential function $f(\phi,\eta)$ has two local minima, $(\phi,\eta) = (0,0)$ and $(\phi,\eta) = (1,1)$. The former is a liquid phase and the latter a crystalline solid. Evolution equations for the three variables are given as

$$\tau_\phi \phi_t = \delta^2\nabla^2\phi + \phi(1-\phi)(\phi-1/2+m) + \eta - \phi - \epsilon^2\phi|\nabla\theta|^2 \tag{3.8}$$

$$\tau_\eta \eta_t = \nu^2\nabla^2\eta + \phi - \eta - 2s\eta|\nabla\theta| \tag{3.9}$$

$$\tau_\theta \eta^2\theta_t = \nabla\cdot\left[s\eta^2\frac{\nabla\theta}{|\nabla\theta|} + \epsilon^2\phi^2\nabla\theta \right] \tag{3.10}$$

Note that the angle variable θ has no meaning in the liquid phase $(\phi,\eta) = (0,0)$.

3.2 2 Dimensional Simulations

We present a 2 dimensional simulations that shows solidification process from nuclei, grain boundary formation by the impingement of crystals and following evolution process including both of the grain boundary motion and grain rotation. Note that in this simulation, the initial values of θ in the liquid phase is set to the dummy value $\theta_{dummy} = -3\pi$. In the vicinity of solid-liquid interface, the value of θ is automatically set by this equation system to the value which equals to the one inside the nearest grain. The following simulation shows partial wetting, *i.e.* grain boundary is wet for the large angle difference and dry for the small difference.

Figure 3.5: Two dimensional simulation of solidification and grain coarsening process. Neumann boundary conditions are imposed on all the variables.

References

[1] R. Kobayashi, J. A. Warren, and W. C. Carter, Physica D, **119**, 415 (1998).

[2] J. A. Warren, W. C. Carter, and R. Kobayashi, Physica A, **261**, 159 (1998).

[3] B. Morin, K. R. Elder, M. Sutton, and M. Grant, Phys. Rev. Lett. **75**, 2156 (1995).

[4] M. T. Lusk, preprint.

[5] L. Q. Chen and W. Yang, Phys. Rev. B **50**, 15752 (1994).

[6] I. Steinbach, F. Pezzolla, B. Nestler, M. BeeBelber, R. Prieler, G.J.Schmitz, and J.L.L. Rezende, Physica D **94**, 135 (1996).

[7] M. T. Lusk, Proc. Royal Soc. London. A, **455** 677 (1999).

[8] R. Kobayashi, J. A. Warren, and W. C. Carter, Physica D, **140**, 141 (2000).

[9] W. C. Carter, J. E. Taylor, and J. W. Cahn J. of Metals, **49**, 30 (1997).

[10] M.-H. Giga, Y. Giga, Arch. Rational Mech. Anal., **141**, 117 (1998).

[11] R. Kobayashi and Y. Giga, J. Stat. Phys., **95**, 1187 (1999).

[12] M.-H. Giga, Y. Giga and R. Kobayashi, Advanced Studies in Pure Mathematics 26, Proc. Taniguchi Conf. on Mathematics, Nara 98, ed. T.Sunada, pp.1-34 (2000)

[13] J. C. M. Li, J. Applied Physics, **33**, 2958 (1961).

[14] H. Hu, Trans AIME, **224**, 75 (1961).

[15] K. E. Harris, V.V. Singh and A. H. King, Acta Mater. **46**, 2623 (1998). (1998).

[16] A. E. Lobkovsky and J. A. Warren, submitted to Physical Review.